Journal of Applied Polymer Science

A comparative study of characteristics of polytetrafluoroethylene fibers manufactured by various processes

Yukang Xu, Chen Huang, Xiangyu Jin
Engineering Research Center of Technical Textiles, Ministry of Education, Donghua University, Shanghai 201620, China
Correspondence to: X. Jin (E-mail: jinxy@dhu.edu.cn)

ABSTRACT: A series of polytetrafluoroethylene (PTFE) fibers were manufactured by three processing methods including extrusion process, split-sheet process and split-film process. The influence of processing methods on fiber properties were systematically studied using four PTFE powders with various molecular weights (3.86×10^7, 4.71×10^7, 4.92×10^7 and 5.11×10^7, respectively). Morphology, crystallinity, tensile behavior and friction properties of PTFE fibers were compared by scanning electron micrograph, X-ray diffraction pattern, strength-elongation curves and friction coefficients, respectively. The results showed that the in terms of flat filaments, mechanical properties became weak with the increase of molecular weight of PTFE powders at first, but were improved dramatically with further enhancement of molecular weight. In the case of both round filaments and split-film fibers, fiber properties were improved with growth of molecular weight. Based on characteristics and friction coefficients, potential applications of three types of PTFE samples were analyzed. © 2016 Wiley Periodicals, Inc. J. Appl. Polym. Sci. **2016**, *133*, 43553.

KEYWORDS: applications; fibers; manufacturing; mechanical properties; textiles

Received 16 September 2015; accepted 16 February 2016
DOI: 10.1002/app.43553

INTRODUCTION

Polytetrafluoroethylene (PTFE) is a polymer with superior chemical inertness, excellent thermal stability,[1] low friction property[2,3] and good biocompatibility.[4–6] On the basis of these outstanding properties, PTFE fibers have been processed into fabrics or felts for further applications such as filtration,[7,8] biomedical products and seawater desalination.[9–11] However, because of the high melt viscosity ($\sim 10^{10}-10^{12}$poise),[12] PTFE fibers cannot be manufactured by the conventional melt spinning technology. At present, PTFE fibers are generally manufactured with paste processing technology, in which, PTFE dispersion powder are firstly mixed with lubricant to form PTFE pastes followed by an extrusion process. The resultant extrudate may be either stretched by rollers, forming round filaments, or rolled and slit to achieve flat filaments by the stretching or carding process with the comb-like needle blade to obtain split-film fibers (also named cotton-like PTFE fibers[13]). Although the processing methods have been well developed, comparative analyses of morphological, structural and mechanical properties of PTFE fibers with different processing methods and various molecular weights (MW) have not been conducted. As the processing technology may largely confine fiber properties and thus affect potential applications,[13–16] a specific comparison of PTFE fibers from different processing paths is critical.

In this study, four types of PTFE virgin dispersion powders with various MW are processed by the above mentioned methods. Scanning electron microscope (SEM) and wide-angle X-ray diffraction patterns (XRD) are used to analyze morphology and crystallinity of fibers. Tensile behaviors, friction coefficients of PTFE fibers and thermal stability of raw powders are also tested, which are employed to deduce the potential application of fibers. The results in our study may not only provide guidance for PTFE fiber manufacture but also help select suitable fibers for end-use products.

EXPERIMENTAL

Materials

PTFE dispersion powders were supplied by Shanghai 3F, Zhonghao Chenguang Chemical Research Institute (Sichuan), Shandong Dongyue and Daikin Fluorine Chemical and the corresponding marks were with the corresponding to MW39 $\times 10^7$, MW47 $\times 10^7$, MW49 $\times 10^7$, MW51 $\times 10^7$ and assigned as MW39, MW47, MW49 and MW51, respectively. Particle average sizes and standard

Additional Supporting Information may be found in the online version of this article.

Table I. Values of S.S.G, Molecular Weight and Average Diameters of Four Powder Samples

Sample	MW39	MW47	MW49	MW51
Average diameter (microns)	0.351	0.370	0.413	0.266
S.S.G	2.172	2.167	2.166	2.165
Mn ($\times 10^7$)	3.86	4.72	4.91	5.11

specific gravity (S.S.G) are listed in Table I. In addition, according to the values of S.S.G, molecular weight of PTFE powders was calculated based on the equation described in ASTM D1457-56T: S.S.G=-0.0579LgMn + 2.6113. The lubricant used in this study was ISOPAR®G from Exxon.

Fibers Manufacture

PTFE fine powders were mixed with lubricant with weight ratio 20:80 to obtain a PTFE powder-lubricant paste. The paste was aged at 35 °C for 24 h to allow a uniform wetting, after which the aged paste was processed into a PTFE preform at room temperature under 4 MPa. Schematic of three fiber formation processes is exhibited in Figure 1. Additionally, fiber formation equipment, namely paste extrusion spun-, slitting sheet filament- and split-film staple fiber-device was purchased from Zixing Dyeing and Finishing Machinery Co. Ltd, China.

PTFE round filament was spun using similar processing procedure described by the literature.[17] The cylindrical PTFE preform with a diameter of 20mm was placed in an extrusion barrel and extruded at a speed of ~10m/min. The temperature was set at 95 °C and the pressure of extrusion was 100 MPa. The 2000μm-diameter as spun PTFE filaments were then drawn by hot-air at 390 °C to reach a drawing ratio of 10. The process is to make PTFE molecular chains orientated along fiber axis and further attenuate the filament to a diameter of ~200μm.

As for PTFE flat filaments with rectangular cross-section, the schematic diagram of manufacture is shown in the middle of Figure 1. In brief, the PTFE paste was compressed into a preform with a diameter of 75 mm. It was then extruded from the spinneret having a diameter of 15 mm under 10 Mpa at ambient temperature. An expanded PTFE sheet having a thickness of about 130 μm was formed by pressing and rolling by a pair of pressure rollers. The PTFE sheet was separated into 24 tapes after passing through a slit roller. Both the rolling and slitting processes were conducted at room temperature. After the treatment of hot-air stretching under 330 °C at the drawing ratio of 10, the unsintered PTFE tape was heated and stretched to the sintered PTFE flat filament with a width of ~1000 μm and a thickness of 90 μm.

During the formation of split-film staple fibers, the expanded PTFE rolled sheet mentioned in the former paragraph was further transported through a series of heating rollers with high temperature (160 °C) to vaporize the lubricants, followed by drawing at 380 °C to form a sintered and uniaxially stretched PTFE film with a thickness of 30μm. Finally, the sintered film went through the processes of splitting and opening with a pair of blade rollers and the comb-like needle blade roller, respectively.

Characterization

ATR-FTIR was operated via a Nicolet 6700 (Thermo Fisher, America) spectrometer. Spectra range was set from 4000 cm^{-1} to 500 cm^{-1}. The analysis of chemical groups in four powders and various PTFE fibers are depicted.

XRD was performed with a D/max-2550PC (Rigaku, Japan) X-ray diffractometer (Cu-Kα radiation with $\lambda = 0.15406$nm operated at 40KV and 35mA). The scan range of 2-theta was from 3° to 60° at a rate of 5°/min. The crystallinity and orientation of PTFE fiber samples were deduced based on the obtained diffraction pattern.

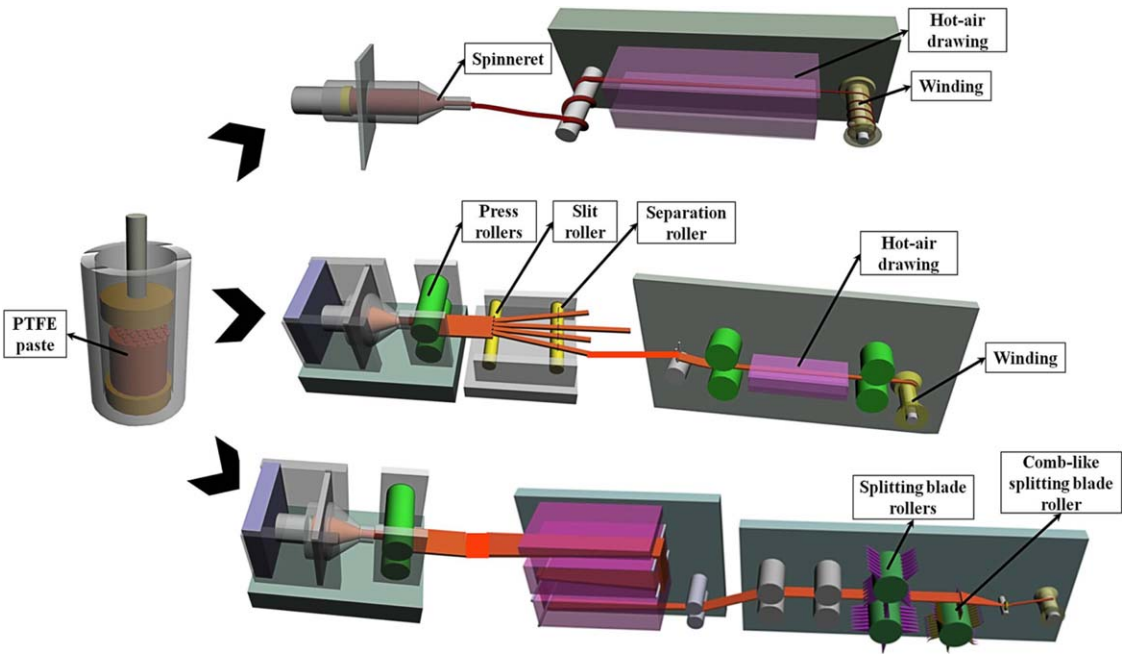

Figure 1. Schematics of three processes of PTFE fibers. [Color figure can be viewed in the online issue, which is available at wileyonlinelibrary.com.]

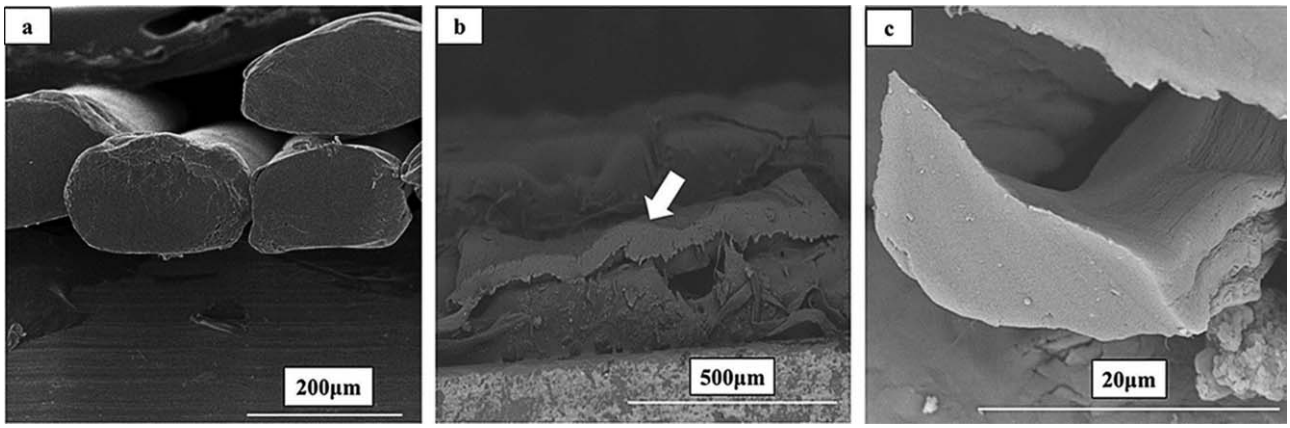

Figure 2. Representative cross sectional view of three types of PTFE fibers, (a) round filament, (b) flat filament and (c) split-film staple fiber. [Color figure can be viewed in the online issue, which is available at wileyonlinelibrary.com.]

Mechanical testing machine (LLY-06, Laizhou China) was employed at a crosshead speed of 10mm/min. the mechanical properties of PTFE fibers were determined and average values were achieved from 20 samples.

Environmental scanning electron microscopy (SEM) (Quanta250, FEI Czekh) was employed to analyze morphologies of PTFE fibers. Samples of filaments or fibers were sputtered with a thin layer of Au to avoid charging, and then imaged using the SEM at 3.5 KV acceleration voltage.[18]

Effective diameter distribution of PTFE flat filament and split-film staple fibers and diameter distribution of PTFE round filaments were analyzed based on the data of widths and diameters obtained by biological microscope (BEION M3, Shanghai Beion Medical Technology Co., Ltd., China).

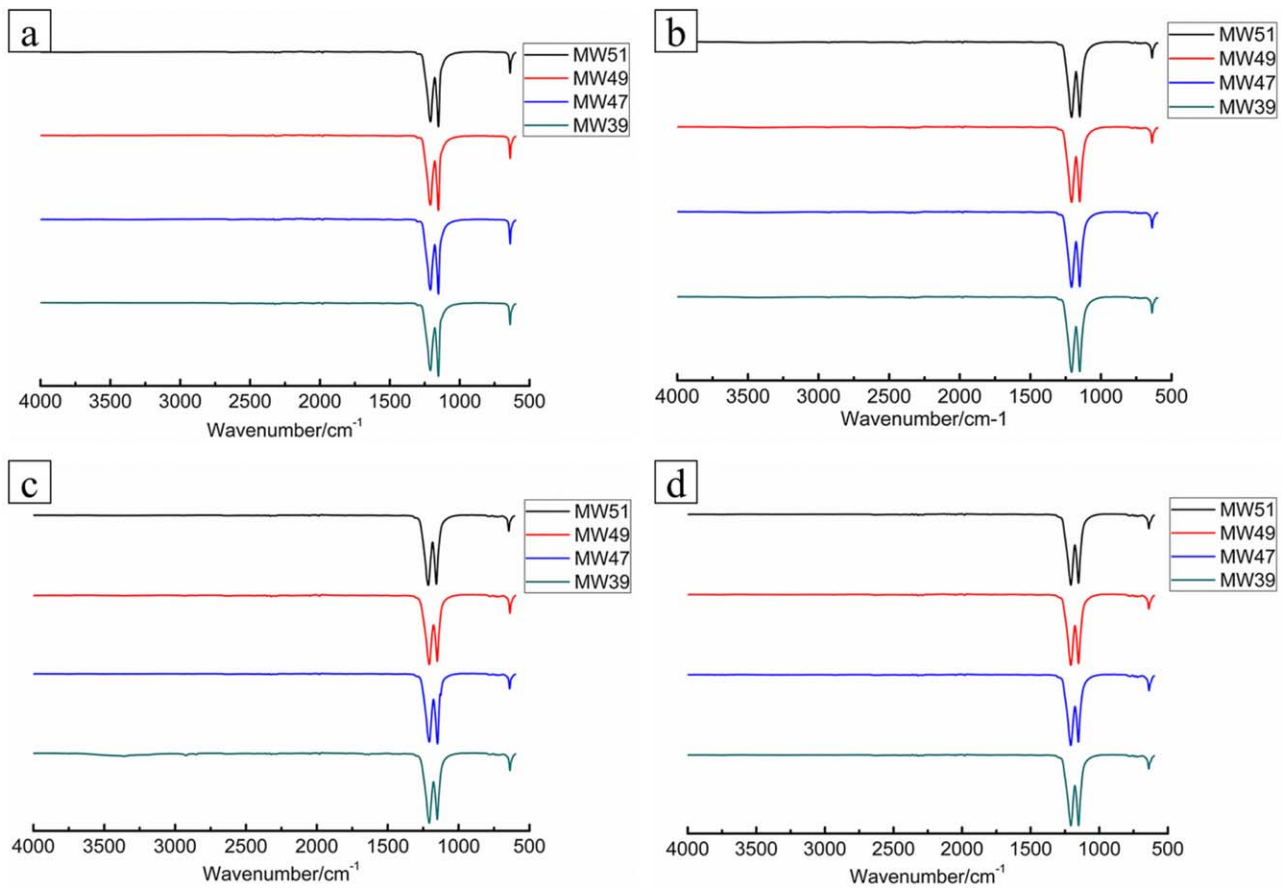

Figure 3. ATR-FTIR spectrum of PTFE dispersion powders and various fibers, (a) dispersion powders, (b) round filaments, (c) flat filaments and (d) split-film fibers. [Color figure can be viewed in the online issue, which is available at wileyonlinelibrary.com.]

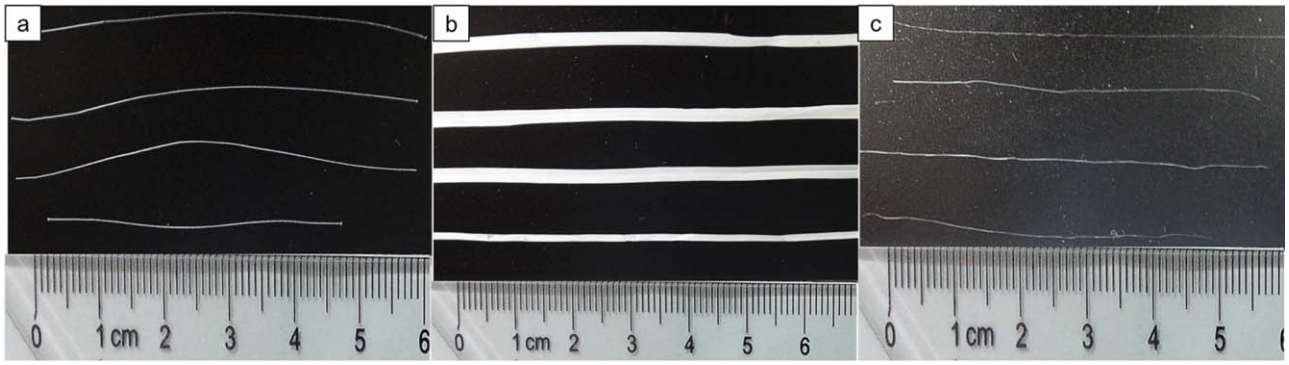

Figure 4. Photos of PTFE fibers from various PTFE powders (I-MW39,II-MW47, III-MW49 and IV-MW51), (a) round filaments, (b) flat filaments and (c) split-film staple fibers. [Color figure can be viewed in the online issue, which is available at wileyonlinelibrary.com.]

The thermal gravimetric analyzer (Q500, TA Instrument Co.,Ltd, United States), set to make the temperature increase from ambient temperature to 800 °C at a rate of 10 °C/min to heat under air atmosphere,[19–21] was adopted to analyze the thermal stability of various PTFE dispersion powder samples respectively.

In addition, frictional coefficients of PTFE fibers were collected by a fiber friction tester (Y151, Donghua University) using the testing procedure developed by Roder.[22] The fiber/metal test method, mentioned by Roder,[22] was employed in this study. During friction test, a cleaned single fiber (taken out from fibers sample randomly) was placed against a small cylinder with the diameter of 1cm, which rotates, at speed of approximately 50rpm, about the horizontal axis. One end of the single fiber was weighed, eliminating the crimp and supporting a required tension, while the other end was attached to a frictional coefficient measuring system, collecting the test results.

RESULTS AND DISCUSSION

Chemical Groups of PTFE Powders and Fibers

ATR-FTIR spectra of PTFE dispersion powder samples and different fibers are shown in Figure 3.

It is clear that the four dispersion powders show the same absorption intensity [Figure 3(a)] that corresponds to two strong peaks (at 1151and 1210cm^{-1}). These peaks could be attributed to the E1 or A2 symmetric stretching vibration of the molecular chains of CF_2 chemical bonds.[23–26] From the spectra, it is reasonable to conclude that the chemical composition of four PTFE powder samples have no significant difference,

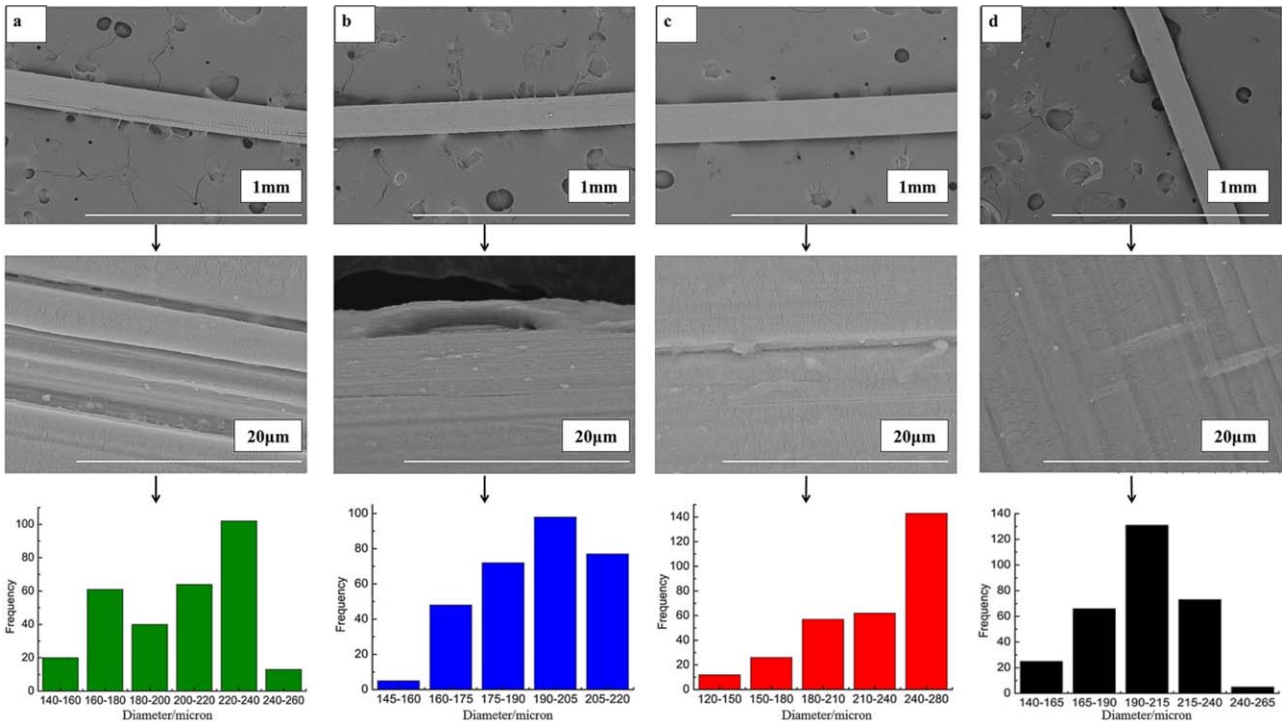

Figure 5. SEM images of round filaments made of different PTFE powders, (a) MW39, (b) MW47, (c) MW49, (d) MW51. [Color figure can be viewed in the online issue, which is available at wileyonlinelibrary.com.]

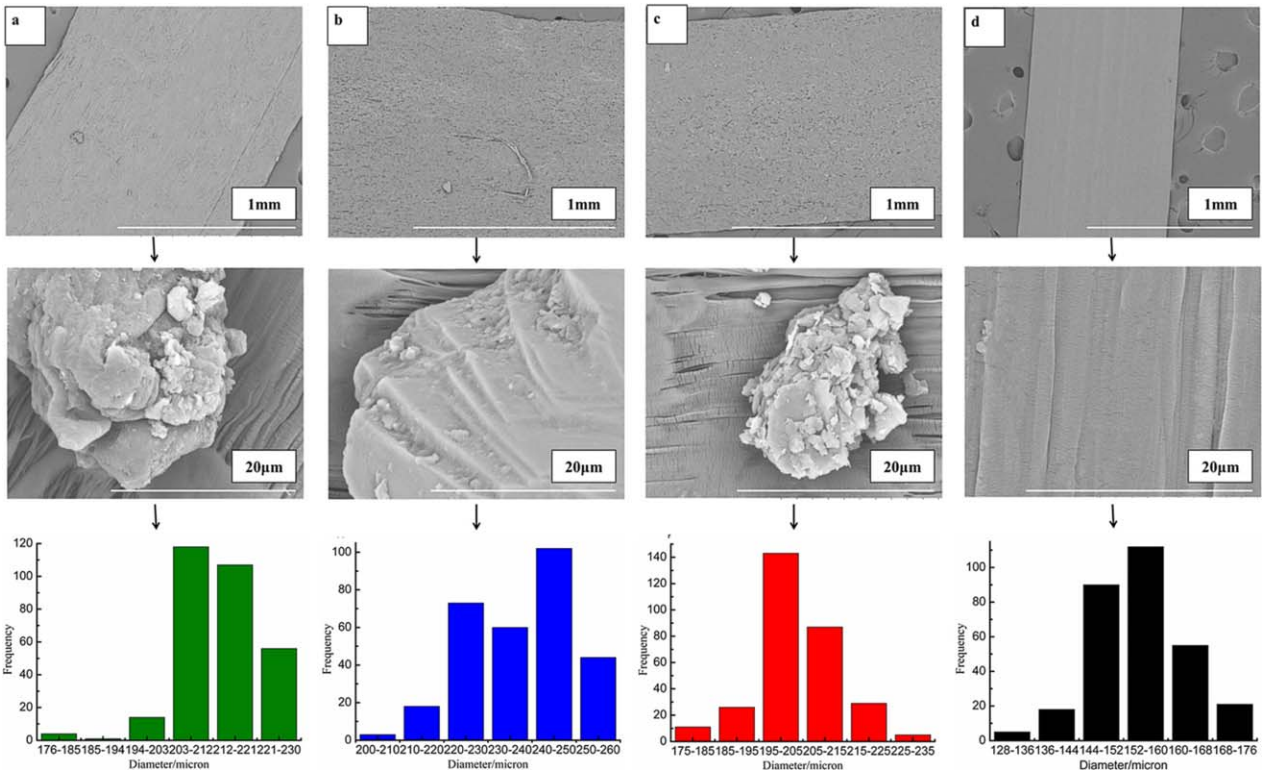

Figure 6. SEM images of flat filaments made of different PTFE powders, (a) MW39, (b) MW47, (c) MW49, (d) MW51. [Color figure can be viewed in the online issue, which is available at wileyonlinelibrary.com.]

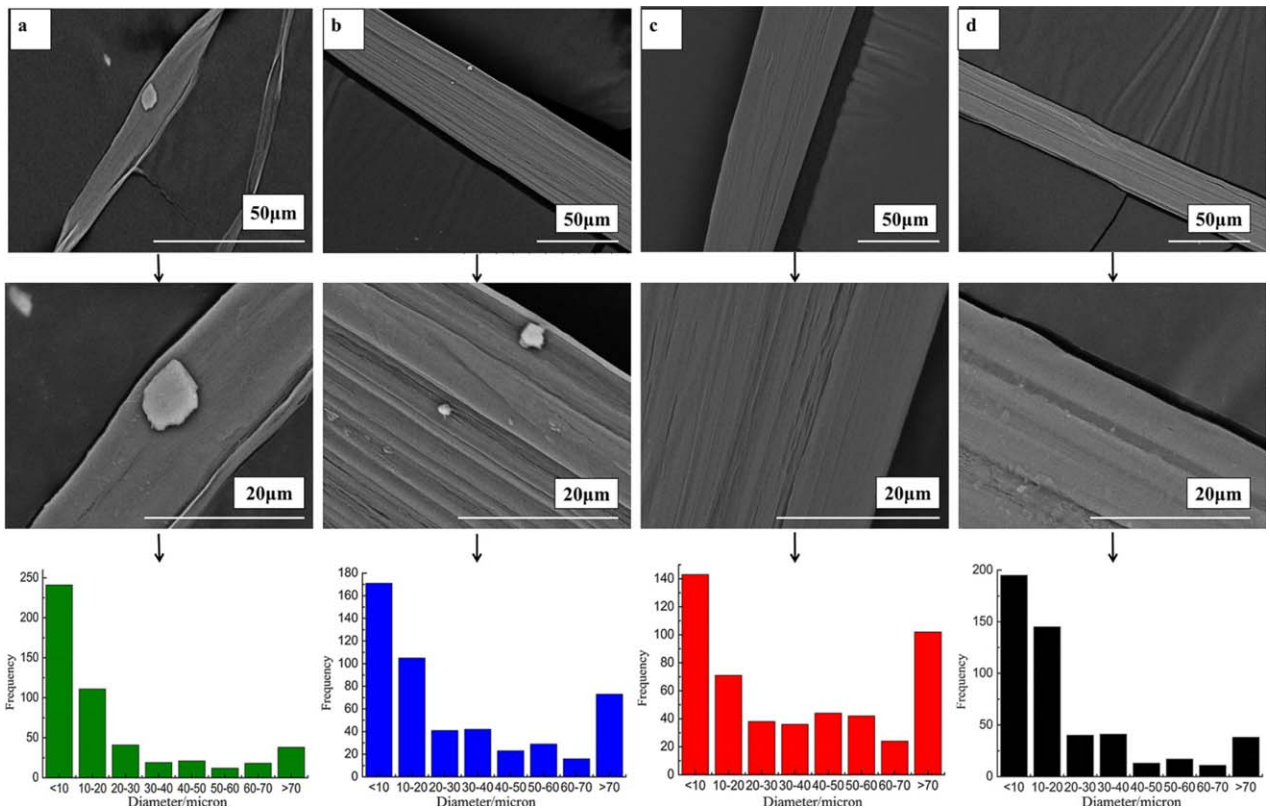

Figure 7. SEM images of split-film staple fibers made of different PTFE powders, (a) MW39, (b) MW47, (c) MW49, (d) MW51. [Color figure can be viewed in the online issue, which is available at wileyonlinelibrary.com.]

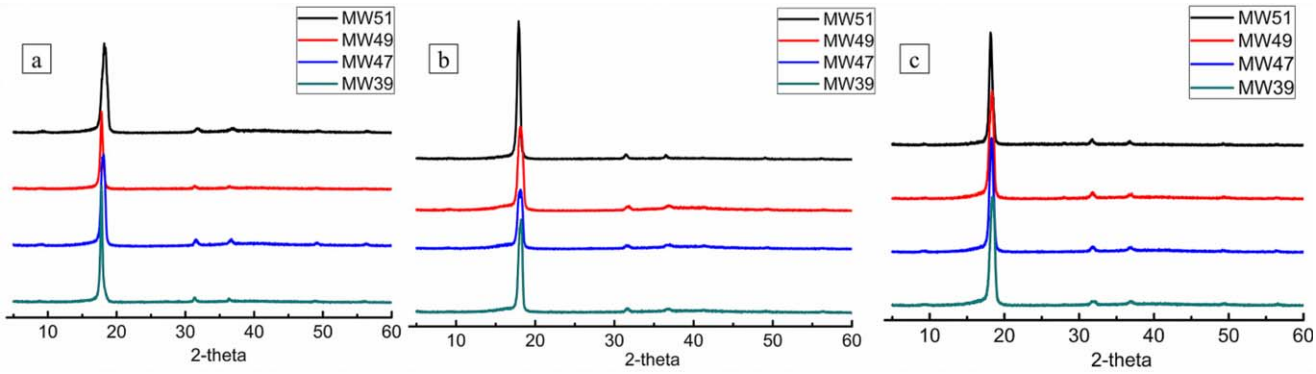

Figure 8. XRD patterns of PTFE fibers made of different PTFE powders, (a) round filaments, (b) flat filaments, (c) split-film staple fibers. [Color figure can be viewed in the online issue, which is available at wileyonlinelibrary.com.]

implying that virgin dispersion powders do not contain extra chemical reagent.

Additionally, absorption intensities of PTFE fibers [Figure 3(b–d)]—produced by the three processing methods showed similar characteristics. Two strong peaks (at 1151 and 1210cm^{-1}), were found in both powder and fiber samples, indicating that there formed no extra component chemical groups formed during fiber manufacturing.

Morphology of PTFE Fibers

The cross shapes of three types of PTFE fibers, namely round filaments, flat filaments and split-film staple fibers, are exhibited in Figure 2. PTFE filaments were manufactured by the spinneret with circular nozzle, which was unlike flat filaments or split-film staple fibers formed by cutting or splitting the films, making flat filaments or staple fibers be provided with rectangular (or like rectangular) cross sections [displayed in Figure 2(b,c), respectively]. Besides, photos of three PTFE fibers from four types of powders were displayed in Figure 4(a–c). It can be clearly found that flat filaments have the maximum width, regardless of the MW of the powders. This is probably because that the PTFE rolled sheet was slit into 24 tapes followed by hot-air drawing process without opening treatment like split-film staple fibers (using needles with microscale diameter). However, the effective diameters of four flat filaments are similar to those of round filaments.

SEM images of the fibers from three processing methods are shown in Figures 5–7, respectively.

For round filaments, it can be observed from Figure 5 that there are many grooves on the surface fibers. For fibers manufactured with MW49- and MW51-powder, a lower number and smaller size grooves are observed, when compared with those of the fibers from MW39- and MW47- powders. Considering the diameter distributions, round filaments from MW51 powders are more uniform than those from other powders.

As shown in Figure 6, PTFE flat filaments made from powder samples of MW39, MW47 and MW49 have porous microstructures. Some particles were not completely melted during fiber manufacture. These particles aggregated into clumps and attached on the surface of flat filaments. However, the surface of filaments from MW51 powder have smooth surface without any particle clumps. This could be explained the conclusion[27] that molecular chains in raw powders were stretched out from crystalline area and formed fine fibrils during the extrusion process. Besides, from the aspect of width of flat filaments, the trend could be found that flat filaments manufactured with MW51 powders have the evenest effective diameter distribution. Thus, based on the analysis of surfaces and effective diameter distributions of flat filaments, it could be inferred that PTFE powders with higher MW (5.11×10^7) are more appropriate to be processed into flat filaments than those with lower MW ($\leq 4.91 \times 10^7$).

Due to the splitting and opening process with needle blade rollers, diameters of PTFE split-film staple fibers are in a wide range from 0.5 to 200μm (Figure 7). Average diameters of fibers made of MW39, MW47, MW49 and MW51 powders are 22.8-, 31.9-, 40.5- and 22.8-microns, respectively. What's more, we find that the number of fibers with diameter $\leq 30\mu$m from MW39- and MW51-powders is larger than that those made of MW47- and MW49-powders. Microgrooves and particles clumps could also be found on split-film staple fiber surfaces. This is probably due to the fact that during the formation of

Table II. Crystallinity, Tensile Behaviors, and Friction Coefficients of Various PTFE Fibers

	Round filaments				Flat filaments				Split-film staple fibers			
Properties	MW39	MW47	MW49	MW51	MW39	MW47	MW49	MW51	MW39	MW47	MW49	MW51
Crystallinity (%)	50.1	56.4	59.8	60.1	54.3	51.2	48.9	56.1	53.4	62.9	65.6	65.8
Strength (cN)	1125	1329	1378	1430	1081	950	852	1518	16.90	20.70	21.40	26.35
Elongation (%)	2.29	3.58	3.03	3.98	7.16	9.85	12.50	6.10	22.70	26.90	28.60	29.2
Friction	0.0874	0.0691	0.0425	0.0853	0.4228	0.3434	0.3627	0.2370	0.4820	0.4413	0.3941	0.2997

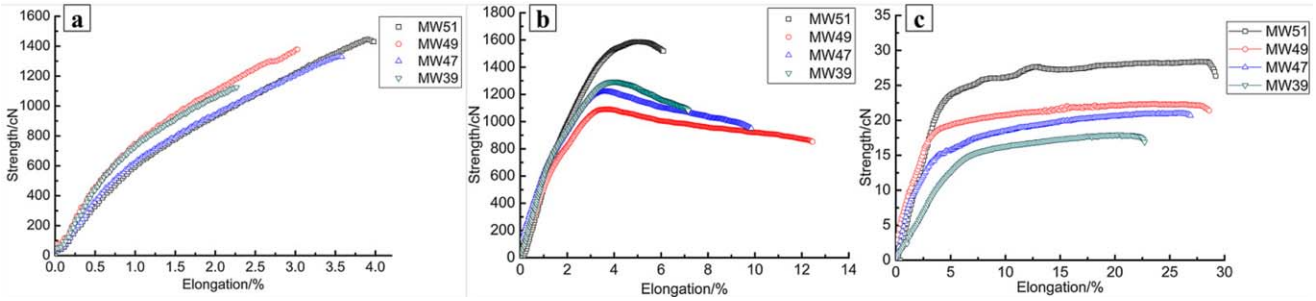

Figure 9. Experimental strength-elongation curves of PTFE fibers manufactured by three processing methods with various MW of raw powder, (a) round filaments, (b) flat filaments, (c) split-film fibers. [Color figure can be viewed in the online issue, which is available at wileyonlinelibrary.com.]

split-film staple fibers before splitting and opening, the uneven drawing force made a few PTFE molecular chains slide and fold. Grooves and particle clumps can be observed from the surfaces of split-film staple fibers produced from MW39- and MW47-powders, while in fibers made of the other powders, the number and size of slots and particle clumps are much less. This phenomenon is possibly attributed to the fact that at same hot-drawing speed, the position of shorter molecular chains may be changed easily compared with longer molecular chains, resulting in irregular molecular arrangements and uneven surface morphologies.

On the basis of morphological characteristics and diameter distributions, fibers from MW51 powders have the best morphology and should be regarded as the ideal candidate for further usage.

Crystallinity of PTFE Fibers

Crystallinity of fibers is estimated quantitatively by XRD.

As shown in Figure 8, the sharp peak at ~18° can be observed from all the samples, implying that the (100) lattice plane had an excellent long-range ordering. The ratio between the crystalline peaks at around 18° and the total peak area was calculated to infer the crystallinity of PTFE fibers. Correspondingly, the deduced values of crystallinities are shown in Table II. Crystallinities of split-film staple fibers are the highest among three types of fibers, whereas those of flat filaments are the lowest, except for fibers from MW39 powders. These results may be attributed to the different processing methods. During the processes of sintering and hot-air drawing, the wide rolled sheets could protect ordered areas of molecular areas from stretching force in the formation of split-film staple fibers compared with filaments, resulting in the improvement of crystallinities.

For flat filaments, the crystallinity ranging from 48.9% to 56.1% decreases gradually with the length of molecular chains, and then increases dramatically after reaching the minimum. This phenomenon should be attributed to the large MW49 dispersion powders (displayed in Table I). After being mixed with the lubricant, the surfaces of the particles in MW49 raw powders were wrapped with a thin layer lubricant. Due to the relatively small specific surface area of large particles, during aging treatment, the amount of lubricant which penetrated into the space between molecular chains in MW49 powders were lower than those of other original powders, resulting in the weak sliding ability of PTFE molecular chains and the low crystallinity in flat filaments.

As for crystallinity in round filaments and split-film staple fibers, crystallinity rises slowly with MW, from 50.1% to 60.1% and 53.4% to 65.8%, respectively. On the one hand, with growth of MW, the long-term order degree of long molecular chains are better than that of short chains mentioned above after cooling slowly from hot drawing. On the other hand, there are no significant growths of crystallinities if MWs increase further, as exhibited in Figure 8 and Table II. This phenomenon can be explained by the fact that the long range ordered degrees could increase firstly with the rise of PTFE molecular chains, but the decrease of sliding ability and increase of cross-linking entanglement of longer molecular chains limit the further enhancement of long-range ordered molecular chains. Thus, it can be concluded that MW51 powders are suitable to be processed into filaments and split-film staple fibers and in view of round filaments and split-film staple fibers, MW49 is also a good choice.

Tensile Behaviors of PTFE Fibers

Tensile behaviors of PTFE fibers are shown in Figure 9(a–c) and the corresponding strengths and elongation ratios at break are recorded in Table II. Evidently, compared with round filaments and flat filaments, PTFE split-film staple fibers have the lowest strengths and elongations to break, as shown in Figure 9 and

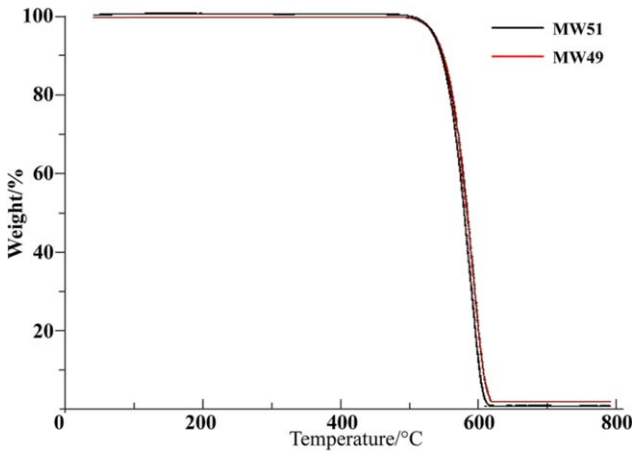

Figure 10. Thermal gravimetric characteristics of MW49-and MW51-PTFE dispersion powders. [Color figure can be viewed in the online issue, which is available at wileyonlinelibrary.com.]

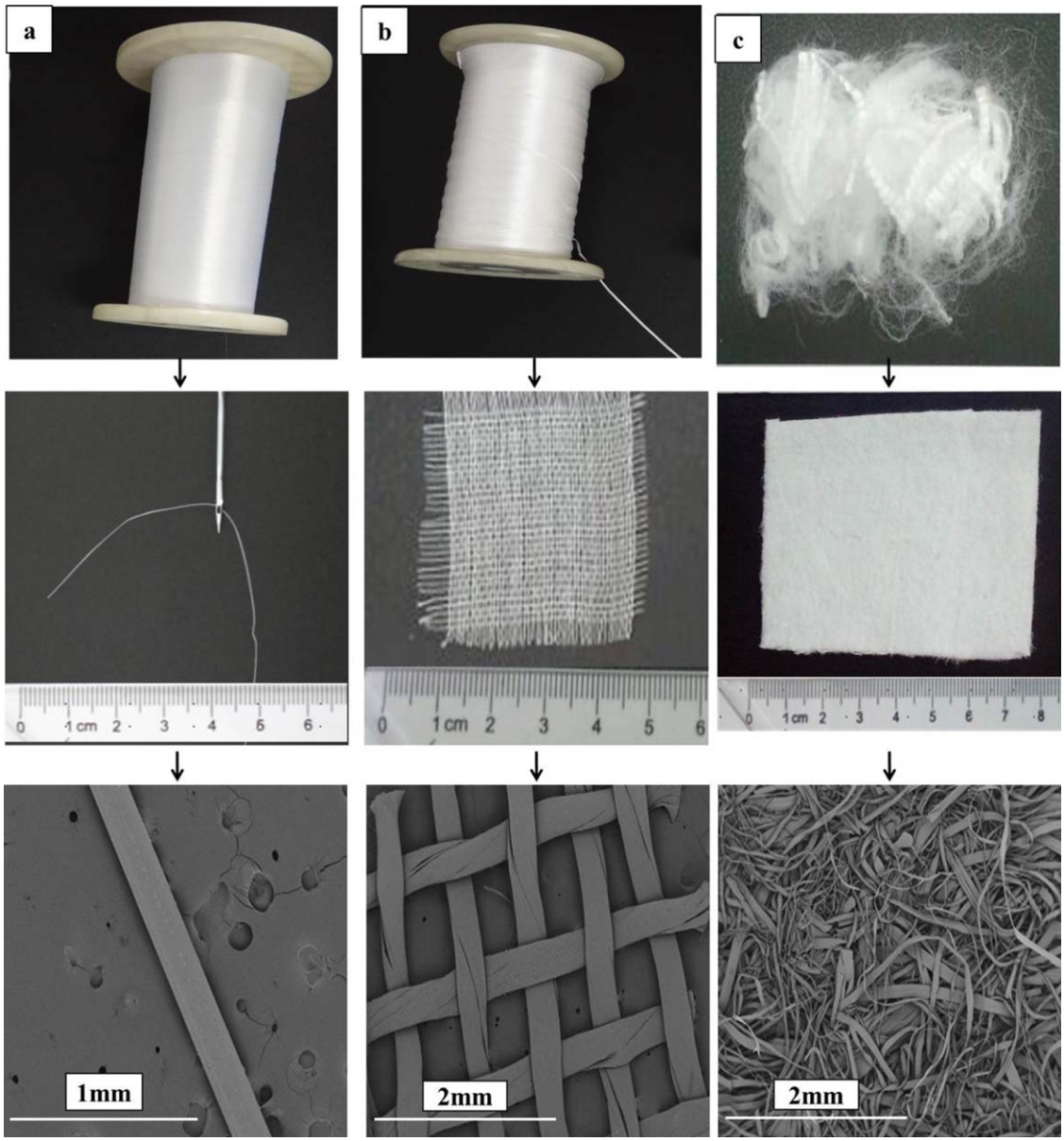

Figure 11. Photos and SEM images of three types of PTFE fibers and products, (a) flat filaments, (b) round filaments and (c) split-film fibers. [Color figure can be viewed in the online issue, which is available at wileyonlinelibrary.com.]

Table II. Considering the similar mechanism of sintering and drawing processes (except for the fiber formation process), the main reason to this result is that the nominal diameters of split-film staple fibers are significantly lower than that of filaments.

In terms of PTFE filaments, it can be found that flat filaments have higher values of elongation ratios at break (7.17%, 9.85%, 12.50% and 6.10% corresponding to the original samples of MW39, MW47, MW49 and MW51powders, respectively) than those (2.29%, 3.58%, 3.03% and 3.98%, respectively) of round filaments. On one hand, this is probably due to the existence of massive micro-pores in flat filaments,[28] which can be seen from Figure 6. Upon being loaded on the tensile tester, the shapes of those micro-pores were stretched along the drawing direction, leading to an extra elongation. Meanwhile, strength to break of flat filaments manufactured from MW51 dispersion powders, 1518cN is much higher than that of round filaments, while in view of filaments made from MW39, MW47 and MW49 powders strengths at breaking of flat filaments are not as high as that of round filaments, implying that MW of virgin powders played a significant role in strength at breaking of PTFE filaments besides of the different methods of fiber formation. On the other hand, significant variance in break elongation ratio between flat filaments and round filaments might be resulted from differences in cross-sectional shape and diameter. Strength of flat filament increased gradually with the increase of elongation and then reaches a peak at 1295cN, 1220cN, 1091cN and 1586cN corresponding to MW39, MW47, MW49 and MW51 flat respectively. However, after passing the maximum, the strength showed a decreased trend with further elongation, as

shown in Figure 9(b). Besides, due to the wide range of fiber diameter, mechanical behavior was affected. The specific correlations between strength/elongation ration at breaking and cross-section shapes or diameters of flat filaments were shown in Supporting Information Figures S1–S3. In the case of round filaments and split-film staple fibers, it is obvious that the break strength increases gradually with MW of starting powders, as exhibited in Figure 9(a,c). Obviously, maximum break strengths for round filament (1430cN) and split-film staple fiber (26.35cN) are both manufactured with MW51 powders displayed in Figure 9(a,c) and Table II. However, for flat filaments, with the growth of MW in virgin powders, the break strength sharply decreases from 1081cN to 895cN first, and then increased to 1518cN [Figure 9(b) and Table II). Therefore, MW51 powders is regarded as favorable to be processed into filaments, as well as split-film staple fibers, and MW49 powders is preferred to be used for round filament because of similar break strengths to those made of MW51 powders. The conclusions inferred by tensile behaviors are consistent with the analyses of XRD.

Friction Coefficients

Friction coefficients of PTFE filaments and fibers are calculated (Table II) to provide significant introduction for potential applications in filtration area. It is found that the friction coefficients of flat filaments and split-film staple fibers are higher than those of round filaments, regardless of MW. In addition, fibers made of MW51 powder show the lowest friction coefficients ($\mu = 0.2370$ and 0.2997, respectively) than other powders. However, the friction coefficient of round filaments declines gradually with the enhancement of MW of PTFE raw powders and then increases. Particularly, round filaments processed with MW49 powders have the lowest friction coefficient, (0.0425). Based on characteristics of friction coefficients, it is believed that MW49 and MW51 virgin dispersion powders are suitable to be used to manufacture PTFE filaments or fibers for filtration applications.

Potential Applications

In order to confirm the possibility of PTFE products working in high temperature environment, thermal gravimetric properties of MW49- and MW51-dispersion powders are shown in Figure 10 indicating that PTFE has prominent thermal stability. Given that the decomposition temperatures of MW49- and MW51-powder are both over 500 °C (593.6 °C and 587.5 °C respectively), the materials could be applied in harsh working environment with high temperature and strong corrosive ability. Due to the high strength (1378cN) and low friction coefficient (0.0425), round filaments, particularly MW49 fibers [as shown in Figure 11(a)], are preferred to be used as sewing threads in industrial applications.[29] In terms of flat filaments, owing to the excellent mechanical and frictional properties, fibers can be woven to the bearing cloth.[16,30] In this study, PTFE flat filaments made of MW51 powders were woven into the fabric [exhibited in Figure 11(b)] with excellent stability that could be used as the bearing cloth in PTFE nonwoven filtration materials. As for split-film staple fibers, the unique cotton-like shape enables the fibers to be readily processed into nonwoven filters.[13] In the present work, the roller card machine and the hydroentanglement device were applied to card split-film staple fibers manufactured with MW51 powders, forming a fiber web [shown in Figure 11(c)] with prominent structural stability, respectively, potentially applied to anti-corrosion and high temperature filtration.

CONCLUSIONS

Various PTFE fibers, namely round filaments, flat filaments and split-film staple fibers, were manufactured by three different processing methods. Fiber morphology, crystallinities and tensile behaviors of PTFE fibers are compared. The results suggest that both filaments and split-film staple fibers made of MW51 virgin powders are ideal to be processed into filaments and split-film staple fibers. Filaments and split-film staple fibers made of MW49 powders show no significant difference with that made from MW51 powders, indicating that MW49 dispersion powders are also preferred to be produced into PTFE filaments and split-film staple fibers. The carded fiber web from split-film staple fibers, bearing clothes fabricated from flat filaments and sewing threads (round filaments) are necessary to manufacture the industrial nonwoven filters.

ACKNOWLEDGMENTS

This work was completed with the help from Linflon New-Materials Technology Co., Ltd (China) and was supported by National Natural Science Foundation of China (51403033), the Fundamental Research Funds for the Central Universities (2232014D3-15) and the Doctoral Fund of Ministry of Education of China (CUSF-DH-D-2015012).

REFERENCES

1. Shulga, Y. M.; Vasilets, V. N.; Kiryukhin, D. P.; Voylov, D. N.; Sokolov, A. P. *RSC Adv.* **2015**, *5*, 9865.
2. Burris, D. L.; Sawyer, W. G. *Wear* **2006**, *261*, 410.
3. Opala, A.; Ziegler, R. U.S. Patent 8,878,851 (**2014**).
4. Xiang, D.; Shan, K. *Wear* **2006**, *260*, 1112.
5. Sawyer, W. G.; Freudenberg, K. D.; Bhimaraj, P.; Schadler, L. S. *Wear* **2003**, *254*, 573.
6. Vashist, M. G.; Singhal, N.; Verma, M.; Sen, J. *Ind. J. Surg.* **2014**, *77*, 1077.
7. Wimmer, A. *Filter Sep.* **1999**, *36*, 26.
8. Zhong, W.; Yu, Y.; Du, C.; Li, W.; Wang, Y.; He, G.; Xie, Y.; He, Q. *RSC Adv.* **2014**, *4*, 40019.
9. Wang, F.; Li, J.; Zhu, H.; Zhang, H.; Tang, H.; Chen, J.; Guo, Y. *Desalination* **2014**, *354*, 143.
10. Hou, D.; Dai, G.; Fan, H.; Huang, H.; Wang, J. *J. Membr. Sci.* **2015**, 476.
11. Shim, W. G.; He, K.; Gray, S.; Moon, I. S. *Sep. Purif. Technol.* **2015**, *143*, 94.
12. Borkar, S.; Gu, B.; Dirmyer, M.; Delicado, R.; Sen, A.; Jackson, B. R.; Badding, J. V. *Polymer* **2006**, *47*, 8337.

13. Tamaru, S.; Yamamoto, K.; Asano, J. U.S. Patent 6,133,165 (**2000**).
14. Silva, R.; Dahl, J. S. U.S. Patent 8,616,110 (**2013**).
15. Fagan, J. P. U.S. Patent 4,031,283 (**1977**).
16. Kelmartin, Jr, T. P.; Roberts, G. M.; Dolan, J. W.; Minor, R. B. U.S. Patent 6,117,547 (**2000**).
17. Mitsoulis, E.; Hatzikiriakos, S. G. *J. Non-Newton. Fluid.* **2009**, *157*, 26.
18. Lei, X.; Yao, P.; Qiao, M.; Sun, W.; Zhang, H.; Zhang, Q. *High Perform. Polym.* **2014**, *26*, 712.,
19. Lei, X.; Qiao, M.; Tian, L.; Chen, Y.; Zhang, Q. *Corros. Sci.* **2015**, *98*, 560.
20. Lei, X. F.; Qiao, M. T.; Tian, L. D.; Yao, P.; Ma, Y.; Zhang, H. P.; Zhang, Q. Y. *Corros. Sci.* **2015**, *90*, 223.
21. Lei, X. F.; Chen, Y.; Zhang, H. P.; Li, X. J.; Yao, P.; Zhang, Q. Y. *ACS Appl. Mater. Interfaces* **2013**, *5*, 10207.
22. Röder, H. L. *J. Text. Inst.* **1953**, *44*, T247.
23. Yilmaz, N. D.; Banks-Lee, P.; Powell, N. B.; Michielsen, S. *J. Appl. Polym. Sci.* **2011**, *121*, 3056.
24. Liang, C. Y.; Krimm, S. *J. Chem. Phys.* **1956**, *25*, 563.
25. Peacock, C. J.; Hendra, P. J.; Willis, H. A.; Cudby, M. E. A. *J. Chem. Soc. A* **1970**, 2943.
26. Li, M.; Zhang, W.; Wang, C.; Wang, H. *J. Appl. Polym. Sci.* **2012**, *123*, 1667.
27. Hatzikiriakos, S. G.; Ariawan, A. B.; Ebnesajjad, S. *Can. J. Chem. Eng.* **2002**, *80*, 1153.
28. Huang, R.; Hsu, P. S.; Kuo, C. Y.; Chung Chen, S.; Lai, J. Y.; Lee, L. J. *Adv. Polym. Tech.* **2007**, *26*, 163.
29. Tamaru, S.; Yamamoto, K.; Asano, J. U.S. Patent 6,416,896 (**2002**).
30. Chou, C.; Huang, J.; Kuo, W. U.S. Patent 0,086,779 (**2005**).